



# A Novel Pyroptosis-Related Signature for Predicting Prognosis and Indicating Immune Microenvironment Features in Osteosarcoma

Yiming Zhang<sup>1†</sup>, Rong He<sup>2†</sup>, Xuan Lei<sup>3</sup>, Lianghao Mao<sup>1</sup>, Pan Jiang<sup>1,4</sup>, Chenlie Ni<sup>1</sup>, Zhengyu Yin<sup>1</sup>, Xinyu Zhong<sup>1</sup>, Chen Chen<sup>5</sup>, Qiping Zheng<sup>5,6\*</sup> and Dapeng Li<sup>1\*</sup>

## OPEN ACCESS

### Edited by:

Frank Emmert-Streib,  
Tampere University, Finland

### Reviewed by:

Junming Ren,  
Stanford University, United States  
Emil Bulatov,  
Kazan Federal University, Russia

### \*Correspondence:

Dapeng Li  
lidapeng706@hotmail.com  
Qiping Zheng  
qp\_zheng@hotmail.com

<sup>†</sup>These authors have contributed  
equally to this work and share first  
authorship

### Specialty section:

This article was submitted to  
Human and Medical Genomics,  
a section of the journal  
Frontiers in Genetics

**Received:** 21 September 2021

**Accepted:** 08 November 2021

**Published:** 26 November 2021

### Citation:

Zhang Y, He R, Lei X, Mao L, Jiang P,  
Ni C, Yin Z, Zhong X, Chen C, Zheng Q  
and Li D (2021) A Novel Pyroptosis-  
Related Signature for Predicting  
Prognosis and Indicating Immune  
Microenvironment Features  
in Osteosarcoma.  
*Front. Genet.* 12:780780.  
doi: 10.3389/fgene.2021.780780

<sup>1</sup>Department of Orthopedics, Affiliated Hospital of Jiangsu University, Zhenjiang, China, <sup>2</sup>Cancer Institute, The Affiliated People's Hospital of Jiangsu University, Zhenjiang, China, <sup>3</sup>Department of Burn and Plastic Surgery, Affiliated Hospital of Jiangsu University, Zhenjiang, China, <sup>4</sup>Guizhou Orthopedics Hospital, Guiyang, China, <sup>5</sup>Department of Hematological Laboratory Science, Jiangsu Key Laboratory of Medical Science and Laboratory Medicine, School of Medicine, Jiangsu University Zhenjiang, Guiyang, China, <sup>6</sup>Shenzhen Academy of Peptide Targeting Technology at Pingshan, and Shenzhen Tyercan Bio-Pharm Co., Ltd., Shenzhen, China

Osteosarcoma is a common malignant bone tumor with a propensity for drug resistance, recurrence, and metastasis. A growing number of studies have elucidated the dual role of pyroptosis in the development of cancer, which is a gasdermin-regulated novel inflammatory programmed cell death. However, the interaction between pyroptosis and the overall survival (OS) of osteosarcoma patients is poorly understood. This study aimed to construct a prognostic model based on pyroptosis-related genes to provide new insights into the prognosis of osteosarcoma patients. We identified 46 differentially expressed pyroptosis-associated genes between osteosarcoma tissues and normal control tissues. A total of six risk genes affecting the prognosis of osteosarcoma patients were screened to form a pyroptosis-related signature by univariate and LASSO regression analysis and verified using GSE21257 as a validation cohort. Combined with other clinical characteristics, including age, gender, and metastatic status, we found that the pyroptosis-related signature score, which we named "PRS-score," was an independent prognostic factor for patients with osteosarcoma and that a low PRS-score indicated better OS and a lower risk of metastasis. The result of ssGSEA and ESTIMATE algorithms showed that a lower PRS-score indicated higher immune scores, higher levels of tumor infiltration by immune cells, more active immune function, and lower tumor purity. In summary, we developed and validated a pyroptosis-related signature for predicting the prognosis of osteosarcoma, which may contribute to early diagnosis and immunotherapy of osteosarcoma.

**Keywords:** osteosarcoma, pyroptosis, prognosis, immunotherapy, survival analysis

## INTRODUCTION

Osteosarcoma is the most common primary aggressive malignancies of the skeleton, and it occurs mainly in children and adolescents, in which distant metastasis still leads to a poor prognosis (Chow et al., 2020; Rojas et al., 2021). With a combination of neoadjuvant chemotherapy, surgery, chemotherapy, and biological therapy in the last few years, the 5-year survival rate for osteosarcoma patients has improved significantly, from 20% to 65–70% (Yao and Chen, 2020; Gazouli et al., 2021). However, due to the limited efficacy of current treatment strategies, nearly 30% of osteosarcoma patients are prone to metastasis or recurrence, with poor prognosis and low 5-year survival rates (Fan et al., 2021). Recently, immunotherapy has undergone a dramatic transformation, demonstrating superior anticancer efficacy in many tumors and being recognized as a more potent and antigen-specific form of antitumor therapy (Constantinidou et al., 2019; Shin et al., 2021). For example, adoptive cellular immunotherapy is a promising option for tumors resistant to current conventional therapy, and chimeric antigen receptor T-cell therapy has been shown to cure 25–50% of patients with previously incurable B-cell malignancies, revolutionizing the treatment of drug-resistant hematologic malignancies (Titov et al., 2021). In addition, specific immune checkpoint inhibitors are being explored as new immunotherapeutic strategies for osteosarcoma, such as CTLA-4, LAG3, TIGIT, and PD-1/L1 (Wang S.-D. et al., 2016; Hashimoto et al., 2020; Judge et al., 2020; Park and Cheung, 2020; Ligon et al., 2021). However, cancer immunotherapies, including checkpoint inhibitors, have varying response rates due to multiple primary and acquired resistance mechanisms (Bashash et al., 2021). In order to improve the early diagnosis and treatment of osteosarcoma, novel biomarkers and therapeutic targets are needed.

Pyroptosis is a newly discovered form of programmed cell death that is morphologically distinct from apoptosis and necrosis while releasing inflammatory mediators in the process (Wu et al., 2021). Pyroptosis is mediated by pore-forming proteins, such as the gasdermin family, of which gasdermin D (GSDMD) is a primary substrate for the caspase family (Li L. et al., 2021). After cleavage by activated caspases, the N-terminal fragment of GSDMD oligomerizes in the membrane to form pores, leading to pyroptosis (Lu et al., 2021). Pyroptosis acts as a double-edged sword in cancer. On the one hand, pyroptosis can create a tumor-promoting environment by releasing inflammatory factors; on the other hand, pyroptosis can inhibit tumor occurrence and progression as a form of programmed death (Xia et al., 2019). As research progresses, the impact of pyroptosis-related genes on the proliferation, migration, and invasion of tumor cells becomes increasingly prominent and is strongly associated with cancer prognosis (Ju A. et al., 2021; Lin W. et al., 2021; Shao et al., 2021; Ye et al., 2021). For instance, Tang et al. (2020) reported that pyroptosis inhibited metastasis of colorectal cancer cells through activation of NLRP3-ASC-Caspase-1 signaling by FL118. In another study by Wang Y. et al. (2016), it was found that the NLRP3 inflammasome can promote the proliferation and migration of A549 lung cancer cells

via the caspase-1-IL-1 $\beta$ /IL-18 signaling pathway. Studies have shown that GSDMD was notably upregulated in osteosarcoma compared to normal skeletal tissue as well as associated with drug resistance and prognosis for patients with osteosarcoma (Lin R. et al., 2020). Alternatively, GSDMD expression was significantly downregulated in gastric cancer tissues, which may contribute to the development of gastric cancer through the regulation of cell cycle transition (Wang et al., 2018). However, the mechanism of pyroptosis-related genes in osteosarcoma is still not fully elucidated.

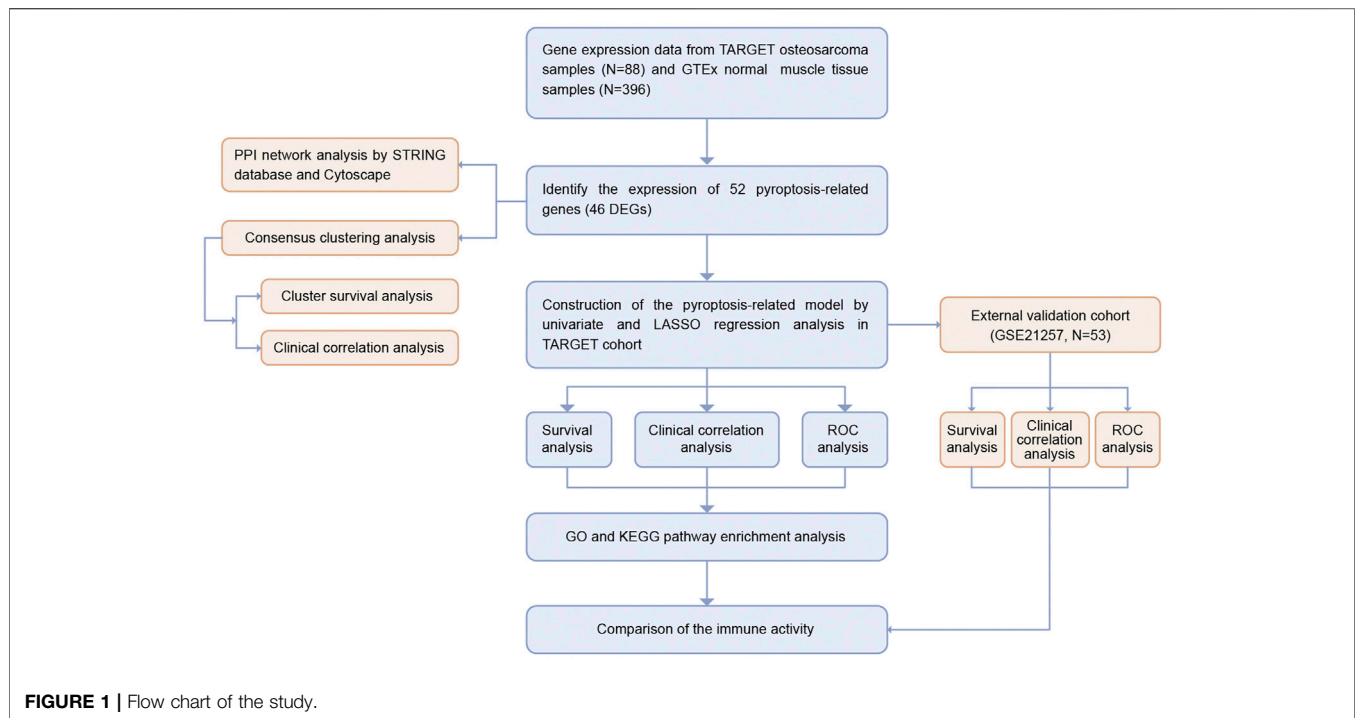
Recently, high-throughput sequencing technologies and bioinformatics analysis have enabled the exploration of genetic alterations in osteosarcoma and provided an effective way to identify potentially beneficial markers and the most appropriate treatment strategies for other cancer types (Li M. et al., 2021; Na et al., 2021; Pan et al., 2021). According to Zhang et al. (Xing et al., 2021), TIMELESS was the most significantly upregulated gene within the 16 clock-related genes by analyzing The Cancer Genome Atlas (TCGA) database and promoted cancer cell proliferation and migration via increasing macrophage infiltration in ovarian cancer. An analysis of the relationship between osteosarcoma development and KIF21B using bioinformatics analysis showed that knockdown of KIF21B inhibited cell proliferation and reduced tumor formation *in vivo* by modulating the PI3K/AKT pathway and that KIF21B was an independent prognostic factor in osteosarcoma patients (Ni et al., 2020). The previous success of projects to identify prognostic target genes suggests that it may be possible to uncover more molecular mechanisms in osteosarcoma.

We used microarray data from the Therapeutically Applicable Research to Generate Effective Treatments (TARGET) and Genotype-Tissue Expression (GTEx) database for differential expression analysis and identified 46 differentially expressed pyroptosis-related genes (DEPRGs) in osteosarcoma and normal muscle tissues. We then constructed a six-gene signature (that could determine the PRS-score) based on DEPRGs to predict osteosarcoma outcomes. We validated the signature by evaluating the association between the PRS-scores and clinical characteristics and immune microenvironment features in osteosarcoma tumors. The differential genes among the PRS-score-based subgroups are also enriched for immunological functions and may be involved in regulating the composition of the immune microenvironment. These results reveal that the pyroptosis-related prognostic signature may provide new insights into osteosarcoma diagnosis and prognosis prediction.

## MATERIALS AND METHODS

### Data Acquisition

The workflow chart of this study is shown in **Figure 1**. We extracted the RNA sequencing (RNA-seq) data and the corresponding clinical information of 88 osteosarcoma patients from the TARGET database (<https://ocg.cancer.gov/programs/target>). The RNA-seq data of 396 normal human muscle tissue samples were obtained from the GTEx database (<https://>



xenabrowser.net/datapages/). Both data types were HTseq-FPKM, and all gene expression levels were processed with  $\log^2$  (FPKM + 1). The independent cohort GSE21257, which contained 53 osteosarcoma samples, was downloaded from Gene Expression Omnibus (GEO) database (<https://www.ncbi.nlm.nih.gov/geo/query/acc.cgi?acc=GSE21257>).

## Identification of DEPRGs

We obtained 52 pyroptosis-related genes (PRGs) from prior reviews (Xia et al., 2019; Zhou and Fang, 2019; Li et al., 2020; Ju X. et al., 2021; Wu et al., 2021; Ye et al., 2021) and MSigDB database v7.4 (Subramanian et al., 2005) (listed in **Supplementary Table S1**). We identified DEPRGs between tumor and normal tissues using the “limma” package, with a  $p$ -value < 0.05. A protein-protein interaction (PPI) network of all DEPRGs was obtained by STRING database (<http://www.string-db.org/>). We used Molecular Complex Detection (MCODE), a plugin for Cytoscape, to cluster the genes and find a densely connected area based on the following criteria: degree cut-off = 2, haircut on, node score cut-off = 0.2, Max depth = 100, k-score = 2, score  $\geq$  5, and node  $\geq$  10.

## Consensus Clustering Analysis

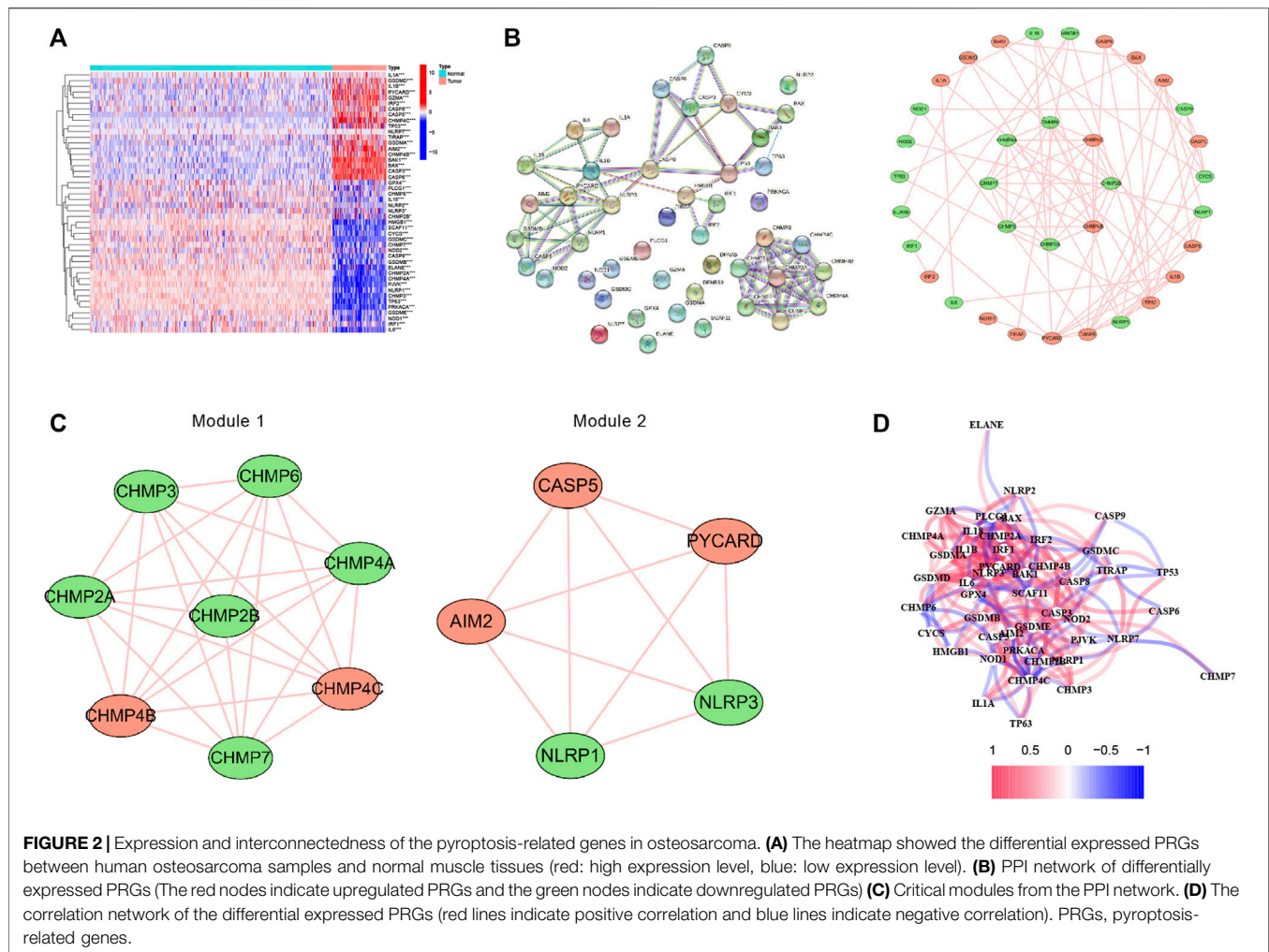
We downloaded all clinical data from the TARGET dataset and further analyzed a total of 85 patients with survival time and status. We performed consensus clustering analysis based on the clinical characteristics of osteosarcoma patients in the TARGET dataset using the “ConsensusClusterPlus” package. The clustering index “k” was increased from 2 to 10 to identify the clustering index with the minor interference and the greatest difference between clusters.

## Construction of a Pyroptosis-Related Scoring Signature

We conducted univariate Cox analysis with the “survival” package to screen for prognosis-related DEPRGs and set 0.1 as the threshold  $p$ -value for omission prevention (Ye et al., 2021). We then conducted the LASSO Cox regression analysis to narrow the risk of overfitting to develop a prognostic signature using “glmnet” package. The TARGET osteosarcoma patients were divided into low and high PRS-score groups based on the median PRS-score, and the PRS-score formula was as follows: PRS-score =  $\sum (\beta_i \times \text{Exp}_i)$  ( $\beta$ : coefficients, Exp: gene expression level). We created a Kaplan–Meier survival curve using the R “survival” and “survminer” packages to determine the OS time between the two subgroups. The principal component analysis (PCA) based on the signature was performed using the R package “Rtsne” and “ggplot2”. The specificity and sensitivity of this prognostic signature were determined by the receiver operating characteristic (ROC) curve constructed with the “SurvivalROC” package. In addition, we identified copy-number alterations and performed mutation analysis of the risk genes in sarcomas using the cBioportal database (<http://www.cbioportal.org/>). Additionally, 53 osteosarcoma patient samples from the GSE21257 dataset were used to verify the reliability of the prognostic model.

## Independent Prognostic Analysis and Clinical Correlation Analysis

We extracted clinical information (gender, age, and metastasis status) of patients in the TARGET cohort. We implemented the “survival” package to conduct both univariate and multivariate



Cox regression analysis to assess the independence of the PRS-score from other clinical variables. The R “RMS” package was then used to generate nomograms to predict survival in patients with osteosarcoma over the course of 1, 3, and 5 years. Additionally, osteosarcoma patients were divided into two subgroups according to age ( $\leq 18$  or  $> 18$  years old), gender (female or male), and metastasis status (M0 and M1). The R “Beeswarm,” “limma,” and “pheatmap” package was used to assess the correlation between the PRGs involved in the prognostic signature and clinical parameters mentioned above.

### Functional Enrichment Analyses

We applied the “limma” R package to identify differentially expressed genes (DEGs) in the PRS-score-classified subgroups, with a false discovery rate (FDR)  $< 0.05$  and absolute value of the  $\log_2$  fold change ( $|\log_2FC|$ )  $\geq 1$  as a threshold. We implemented the “clusterProfiler” package to conduct the Gene Ontology (GO) and Kyoto Encyclopedia of Genes and Genomes (KEGG) analysis based on the DEGs between different PRS-score subgroups, with an adjusted  $p$ -value (adj.  $P$ )  $< 0.05$ . Subsequently, the “GSVA”

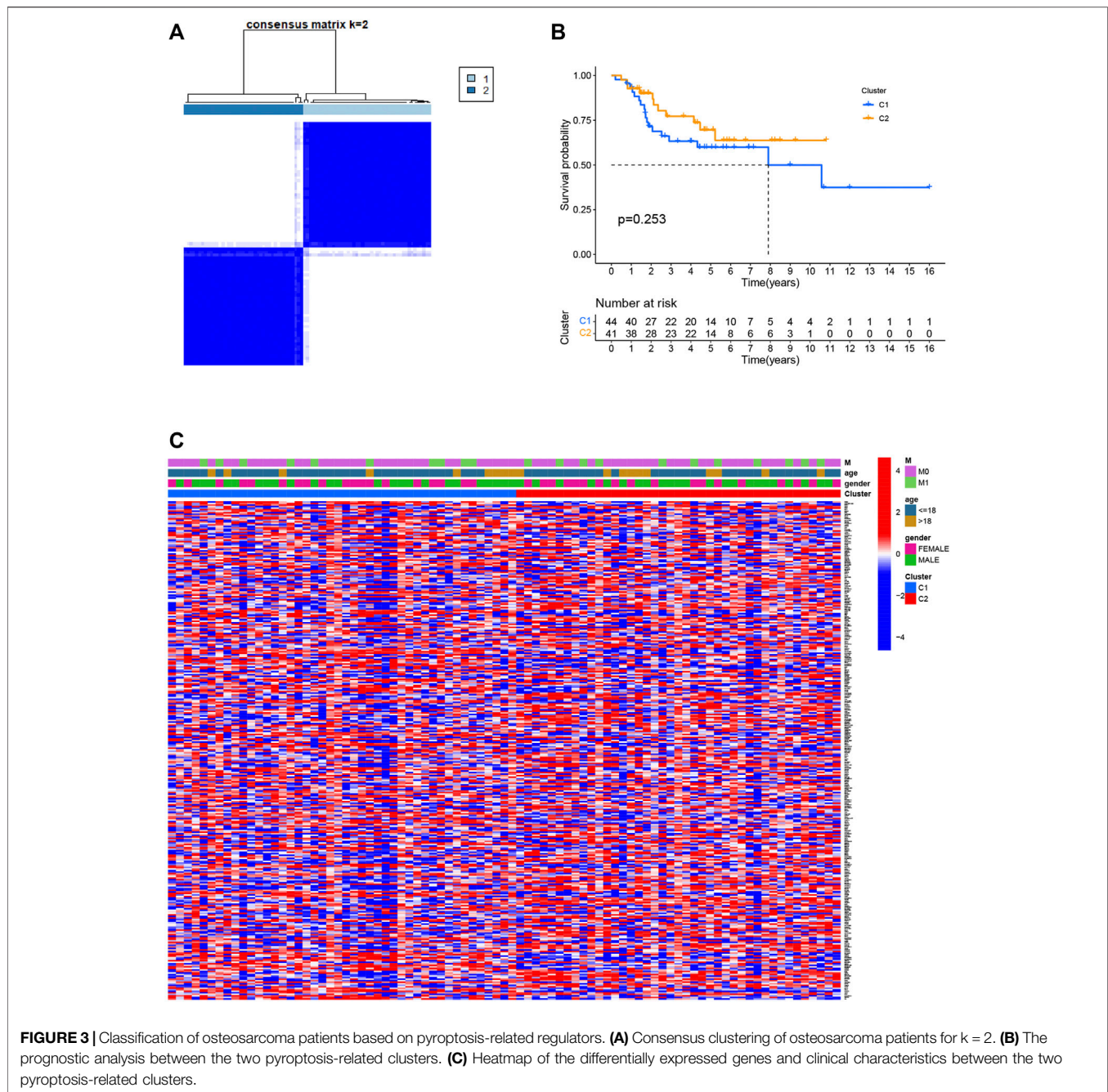
package was used to conduct the single sample Gene Set Enrichment Analysis (ssGSEA) to calculate the enrichment scores of immunological cells and functions.

### Analysis of the Immune Microenvironment Features and Immune Response

Immunoscore and stromal scores for each osteosarcoma patient were obtained using the “estimate” and “limma” packages and were used to derive tumor purity. Using the “ggpubr” and “limma” packages, we assessed the differential expression of immune checkpoints (CTLA4, PDL1, LAG3, TIGIT, TIM3, PDCD1, IDO1, and TDO2) between subgroups to estimate the predictive power of the signature for immunotherapy response.

### Statistical Analysis

We executed all statistical analyses with R software (v4.0.5). The threshold for statistical significance was taken as  $p < 0.05$  if it was not explicitly stated.



## RESULTS

### DEPRGs in Human Osteosarcoma and Normal Tissues

The expression levels of 52 PRGs were compared in the human osteosarcoma samples and normal muscle tissues, and we detected 19 DEPRGs that were upregulated and 27 DEPRGs that were down-regulated using our threshold criteria ( $p$  value  $< 0.05$ ) (Figure 2A). The PPI network of DEPRGs created with the minimum required interaction score  $> 0.9$  is presented in Figure 2B. We then screened out the two most crucial

network modules using MCODE (Figure 2C) and drew the correlation network of the differentially expressed PRGs (Figure 2D).

### Identification of Subgroups Based on PRGs by Consensus Clustering

Consensus clustering was used to separate all 85 osteosarcoma patients into subgroups according to the expression of PRGs. By increasing the clustering index “ $k$ ” from 2 to 10, we found that  $k = 2$  seems to be the optimal point to identify the smallest

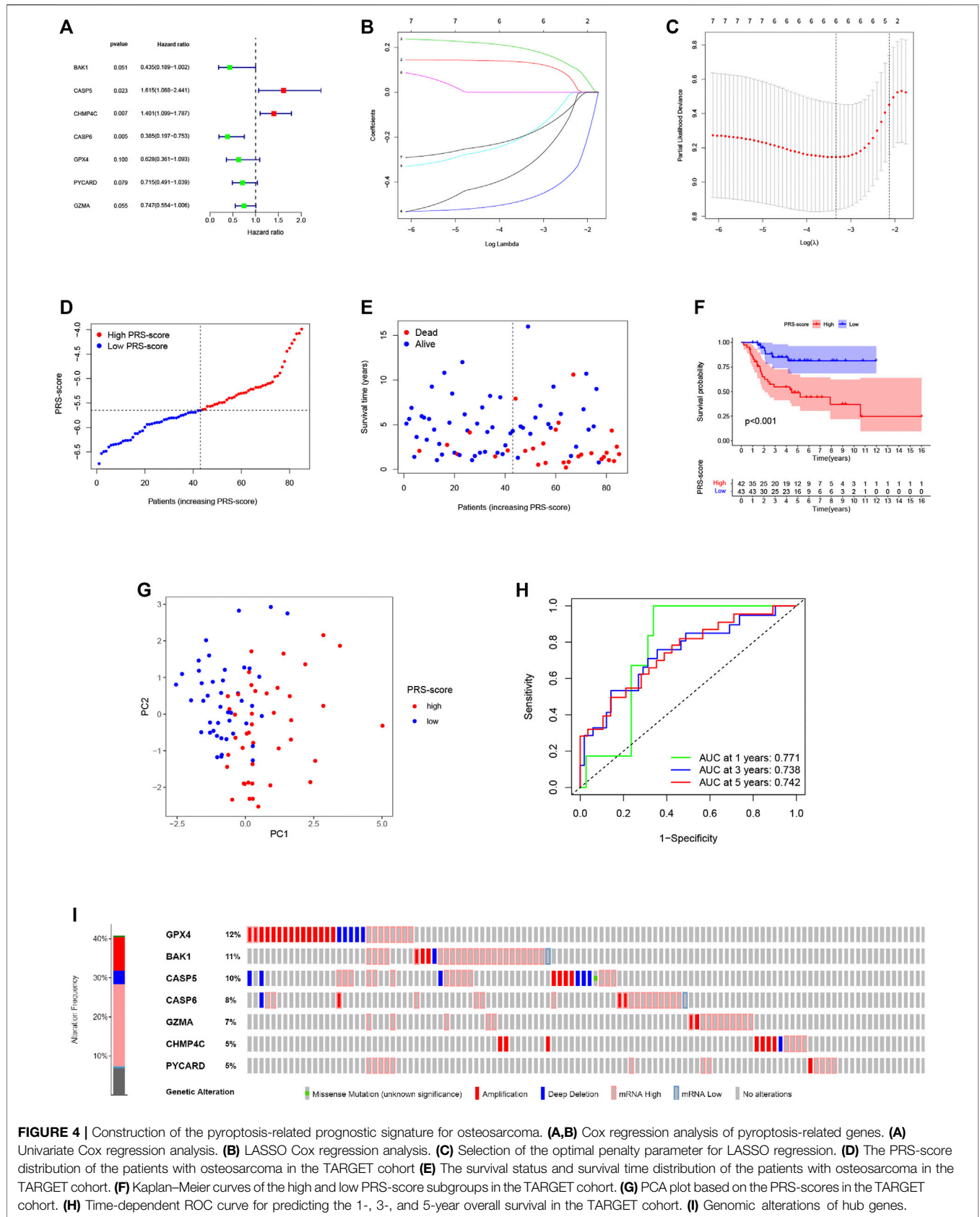
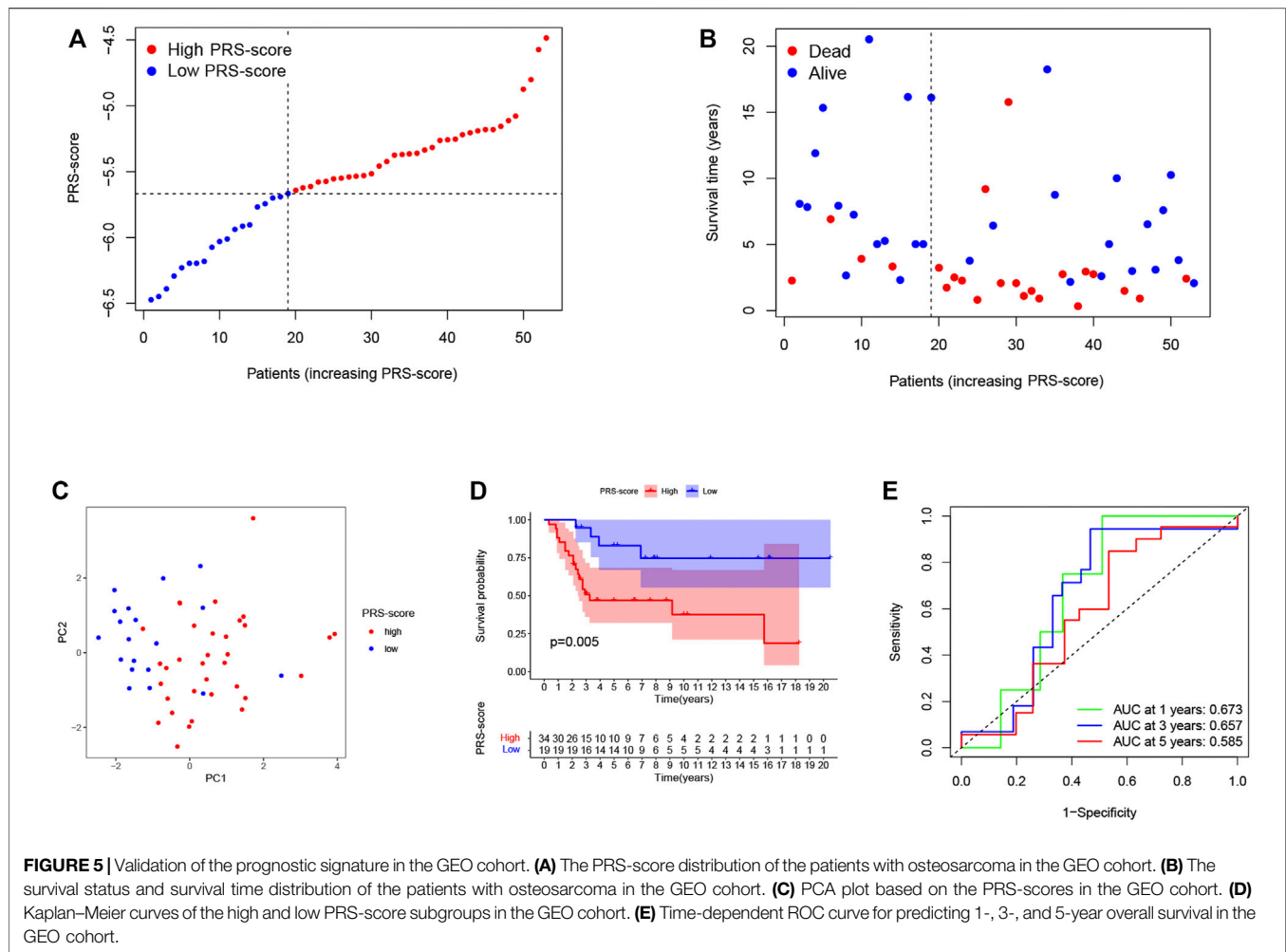


**FIGURE 4 |** Construction of the pyroptosis-related prognostic signature for osteosarcoma. **(A,B)** Cox regression analysis of pyroptosis-related genes. **(A)** Univariate Cox regression analysis. **(B)** LASSO Cox regression analysis. **(C)** Selection of the optimal penalty parameter for LASSO regression. **(D)** The PRS-score distribution of the patients with osteosarcoma in the TARGET cohort **(E)** The survival status and survival time distribution of the patients with osteosarcoma in the TARGET cohort. **(F)** Kaplan-Meier curves of the high and low PRS-score subgroups in the TARGET cohort. **(G)** PCA plot based on the PRS-scores in the TARGET cohort. **(H)** Time-dependent ROC curve for predicting the 1-, 3-, and 5-year overall survival in the TARGET cohort. **(I)** Genomic alterations of hub genes.

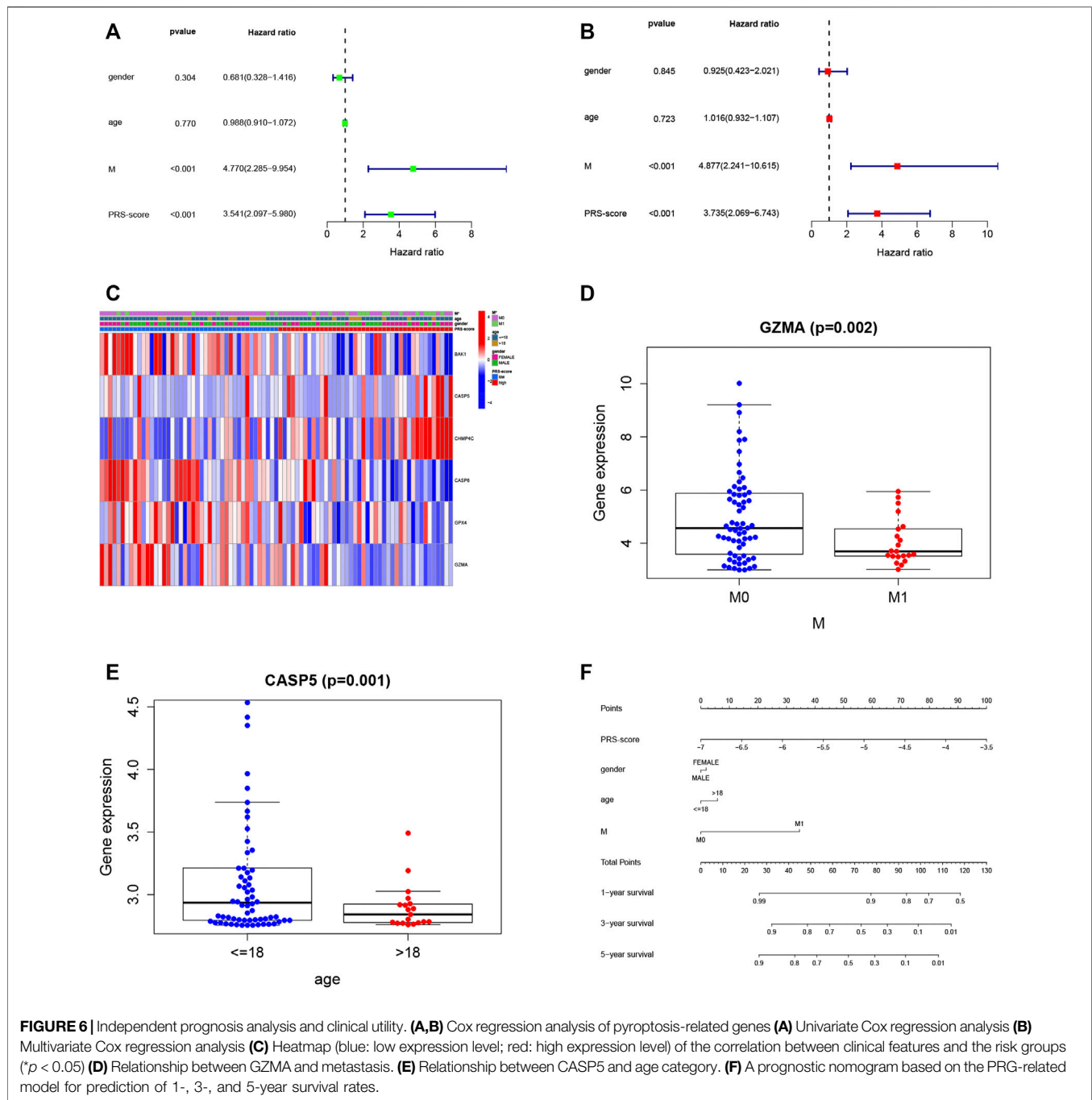


interferences and the most significant differences between clusters (Figure 3A). Consequently, patients with osteosarcoma in the training group were classified into two clusters. However, a comparison of overall survival between the two clusters revealed no significant difference ( $p = 0.253$ , Figure 3B). We also plotted a heatmap to express the differences in gene expression and clinical characteristics, including age ( $\leq 18$  or  $> 18$  years old), gender (male or female), and metastasis status (metastatic, non-metastatic) between the clusters, but we found there are little differences (Figure 3C).

## Construction of the PRG-Based Prognostic Signature

To construct a pyroptosis-related prognostic model, we further screened seven-candidate prognostic PRGs by univariate Cox regression analysis (Figure 4A). Of the seven prognostic PRGs, CASP5 and CHMP4C were regarded as high-risk genes based on their HRs, whereas BAK1, CASP6, GPX4, PYCARD, and GZMA were regarded as low-risk genes. Subsequently, LASSO Cox regression analysis was performed to construct a 6-gene signature

according to the optimum penalty parameter ( $\lambda$ ) value (Figures 4B,C). We then divided the patients in the TARGET cohort into high and low scoring subgroups based on a composite signature score termed the “PRS-score” (PRS-score = [BAK1 expression  $\times (-0.325)$ ] + [CASP5 expression  $\times (0.132)$ ] + [CHMP4C expression  $\times (0.191)$ ] + [CASP6 expression  $\times (-0.475)$ ] + [GPX4 expression  $\times (-0.185)$ ] + [GZMA expression  $\times (-0.185)$ ]). The PRS-scores, survival status, and survival time in the two groups of patients are shown in Figures 4D,E. The results showed that patients with higher PRS-scores had worse prognoses than patients with lower PRS-scores. Kaplan-Meier curves showed that the patients in the high PRS-score group had worse OS than the patients in the low PRS-score group ( $p < 0.001$ ; Figure 4F). Analyses of PCA revealed that high and low PRS-score patients were separated into two clusters (Figure 4G). To assess the accuracy of the signature, we then constructed a time-dependent ROC curve. We found the area under the ROC curve (AUC) was 0.771 for 1-year OS, 0.738 for 3-year OS, and 0.742 for 5-year OS, providing evidence that this six-gene prognostic model performed well as a predictor of OS (Figure 4H). Mutations and copy number alterations of the six hub genes (BAK1, CASP6, GPX4, PYCARD, GZMA, CASP5, and CHMP4C) were analyzed together using the cBioportal database.



These six hub genes were altered in 99 of 241 samples (41%) (Figure 4I). Since the frequency of mutations in GPX4 and BAK1 exceeded 10%, we hypothesized that these two genes might be key therapeutic targets (Figure 4I).

### Validation of the PRG-Based Prognostic Signature

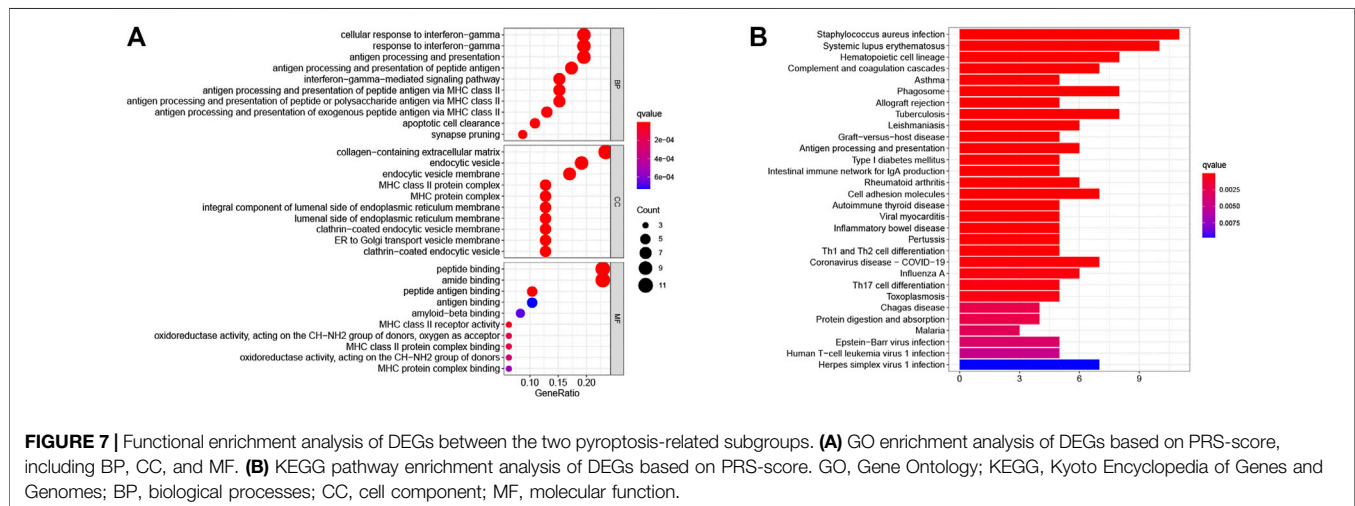
To reliability of this six-gene prognostic signature, a total of 53 patients from GSE21257 were used as the test set. Based on

the median cut-off of the PRS-score in the TARGET cohort, patients with osteosarcoma in the GEO cohort were separated into high ( $n = 34$ ) and low ( $n = 19$ ) scoring groups (Figure 5A). The survival time and survival status distribution showed that patients in the low PRS-score subgroup had a higher possibility of surviving (Figure 5B). The PCA of the two subgroups showed a clear separation (Figure 5C). Furthermore, Kaplan-Meier analysis revealed that osteosarcoma patients with high PRS-scores had a significantly poorer prognosis than those with low PRS-

**TABLE 1** | The relationship between PRS-scores and clinical characteristics.

Id	Gender (female, male) t (p)	Age ( $\leq 18$ , $> 18$ ) t (p)	M stage (M0, M1) t (p)
BAK1	-0.182 (0.856)	1.324 (0.197)	0.091 (0.928)
CASP5	1.257 (0.213)	<b>3.287(0.001)</b>	-0.08 (0.936)
CHMP4C	0.84 (0.404)	1.609 (0.115)	-0.568 (0.574)
CASP6	-0.724 (0.472)	0.128 (0.899)	1.965 (0.056)
GPX4	0.062 (0.951)	0.32 (0.751)	1.664 (0.107)
GZMA	0.341 (0.734)	1.434 (0.160)	<b>3.293(0.002)</b>
PRS-scores	0.742 (0.461)	-0.093 (0.926)	<b>-2.58(0.015)</b>

t, t value from Student's t test; p, p-value from Student's t test. Bold indicates statistical significance,  $p < 0.05$ .



scores (Figure 5D), with AUC = 0.673, 0.657, and 0.585 for 1, 3, and 5 years survival, respectively (Figure 5E).

## Independent Prognostic Value and Clinical Utility of the Prognostic Signature

We then utilized univariate and multivariable Cox regression analyses to evaluate the independent prognostic value of the model with other clinical features. The univariate Cox analysis indicated that the PRS-score (HR = 3.541, 95% CI = 2.097–5.980,  $p < 0.001$ ) and M-stage (HR = 4.770, 95% CI = 2.285–9.954,  $p < 0.001$ ) were significantly associated with OS (Figure 6A). The multivariate Cox analysis confirmed that the PRS-score (HR = 3.735, 95% CI = 2.069–6.743,  $p < 0.001$ ) and M-stage (HR = 4.877, 95% CI = 2.241–10.615,  $p < 0.001$ ) were independent factors affecting the prognosis of osteosarcoma patients (Figure 6B). We then plotted a clinical information-related heatmap for the TARGET cohort and found significant differences in M-stage distribution between low- and high-scoring subgroups (Figure 6C). The results of clinical correlation analysis showed that the M stage of osteosarcoma patients decreased with increasing GZMA expression (Figure 6D,

$p < 0.01$ ), while osteosarcoma patients with high CASP5 expression were younger (Figure 6E,  $p < 0.01$ ), and all results are shown in Table 1. Additionally, a pyroptosis-related signature-based nomogram showed that the OS of patients at 1, 3, and 5 years decreased with increasing PRS-score (Figure 6F).

## Functional Analysis of DEGs Based on PRS-Score

To further investigate differences in PRS-score-classified subgroups, we identified 34 genes that were down-regulated and 14 genes that were up-regulated in the high PRS-score subgroup compared with the low PRS-score subgroup in the TARGET group (Supplementary Table S2). GO analysis revealed that the 48 DEGs were mainly involved in the cellular response to interferon-gamma, MHC class II protein complex, peptide binding, and amide binding (Figure 7A). According to the KEGG pathway analysis, these DEGs were primarily associated with staphylococcus aureus infection, systemic lupus erythematosus, hematopoietic cell lineage, and complement and coagulation cascades (Figure 7B).

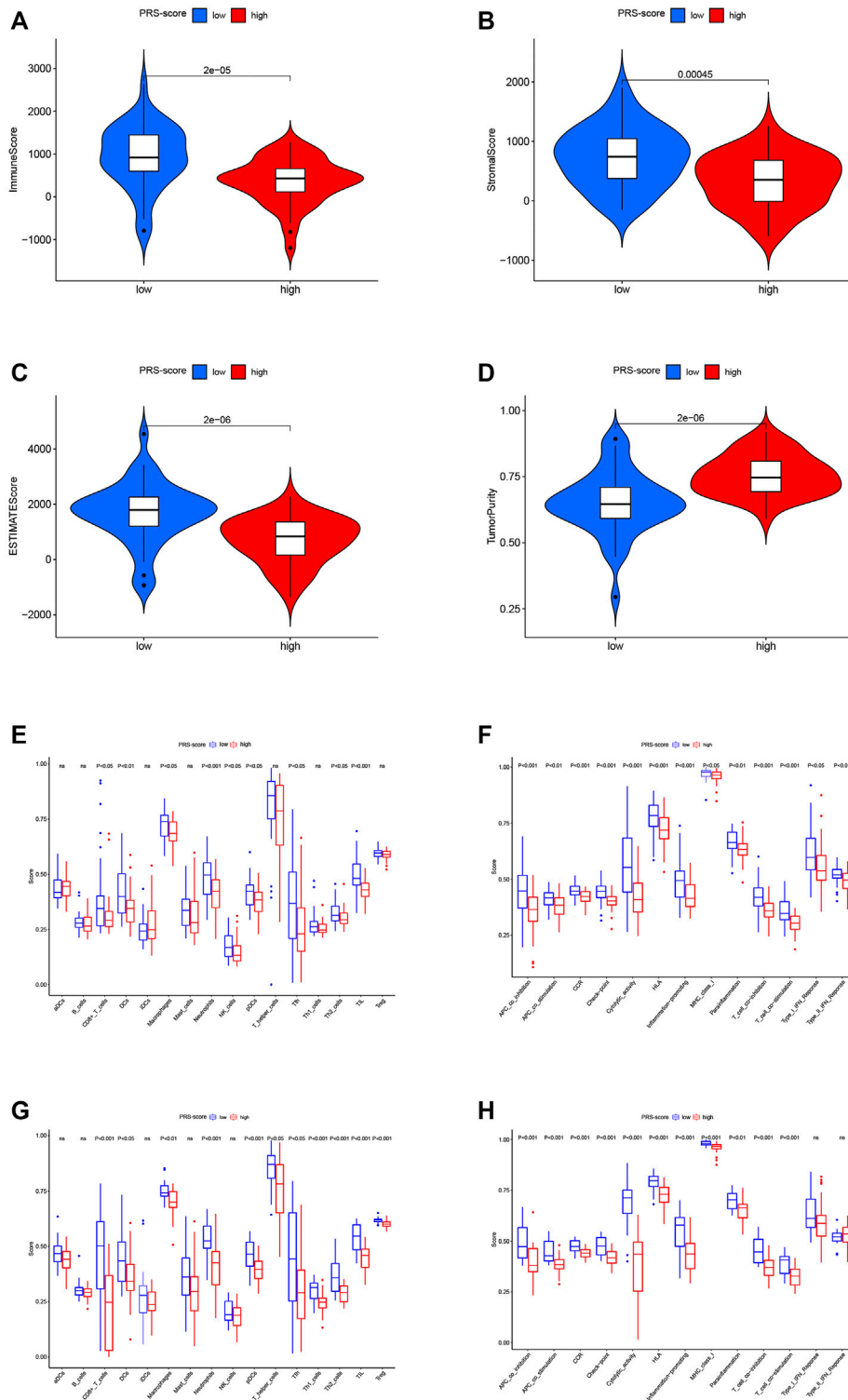
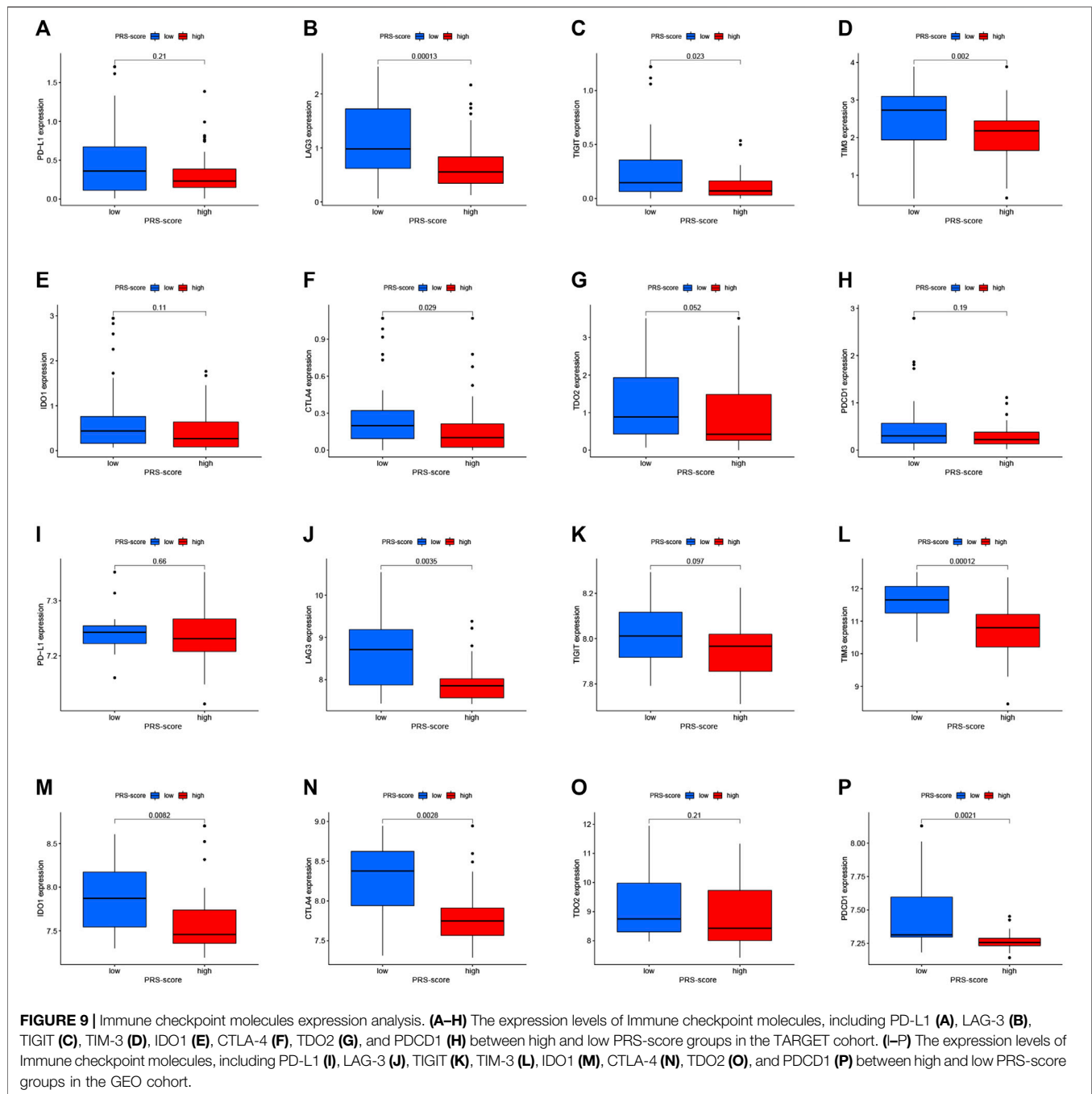


**FIGURE 8 |** Immune characteristics analysis of the prognostic signature. **(A)** Immune scores between high and low PRS-score groups. **(B)** Stromal scores between high and low PRS-score groups. **(C)** ESTIMATE scores between high and low PRS-score groups. **(D)** Tumor purity between high and low PRS-score groups. **(E)** Comparisons of the level of immune cell infiltration between high and low PRS-score groups in the TARGET cohort. **(F)** Comparisons of immune functions between high and low PRS-score groups in the TARGET cohort. **(G)** Comparisons of the level of immune cell infiltration between high and low PRS-score groups in the GEO cohort. **(H)** Comparisons of immune functions between high and low PRS-score groups in the GEO cohort.



## Analysis of Immune Microenvironment Characteristics Between Subgroups

Several studies have shown that the tumor immune microenvironment correlates strongly with malignant behavior; thus, we investigated the unique features of the tumor microenvironment (TME) to distinguish between the two subgroups of patients. Based on the ESTIMATE algorithm, the overall level of immune cell infiltration and tumor purity were examined. As shown in **Figures 8A–D**, the immune score,

stromal score, and ESTIMATE score were significantly higher in the low scoring group than in the high scoring group, while the tumor purity was lower. We then explored the distribution patterns of infiltrating immune cells in different subgroups using the ssGSEA algorithm. In the TARGET cohort, the patients in the high PRS-score group had lower levels of tumor infiltration by CD8<sup>+</sup> T cells, dendritic cells (DCs), macrophages, neutrophils, natural killer cells, plasmacytoid dendritic cells (pDCs), Th2 cells, Tfh cells, and tumor-infiltrating lymphocytes (TILs) compared with the patients in

the low PRS-score group (**Figure 8E**). All 13 immune functions were down-regulated in the patients in the high PRS-score group in comparison with the patients in the low PRS-score group (**Figure 8F**). In the GEO cohort, compared with the patients in the low PRS-score group, the patients in the high PRS-score group had lower levels of tumor infiltration by immune cells, including CD8<sup>+</sup> T cells, DCs, macrophages, neutrophils, pDCs, TILs, T regulatory, Tfh, Th1, and Th2 cells (**Figure 8G**). Moreover, in contrast to the type-1 and type-2 interferon response pathways, the other 11 immune pathways had lower activity in the high PRS-score group than in the low PRS-score group (**Figure 8H**). Our investigation showed that PRS-scores were associated with immune characteristics and that elevated immune activity in the low-scoring samples may contribute to the antitumor effect in osteosarcoma.

In addition, we analyzed the changes in immune checkpoint expression between the high and low PRS-score groups. **Figures 9A–H** shows that in the TARGET cohort, LAG3 ( $p = 1.3e-04$ ), TIGIT ( $p = 0.023$ ), TIM3 ( $p = 0.002$ ), and CTLA4 ( $p = 0.029$ ) expressions were down-regulated in the high-scoring group in comparison to the low-scoring group. On the other hand, as the PRS-score increased, the expression of LAG3 ( $p = 0.0035$ ), TIM3 ( $p = 1.2e-04$ ), IDO1 ( $p = 0.0082$ ), CTLA4 ( $p = 0.0028$ ), and PDCD1 ( $p = 0.0021$ ) in patients with osteosarcoma also decreased in the GEO cohort (**Figures 9I–P**).

## DISCUSSION

Pyroptosis, a form of programmed cell death, was found to play a dual role in both promoting and inhibiting the growth of different tumor cells (Loveless et al., 2021). Several recent studies have highlighted the relevance of pyroptosis-related genes as candidate biomarkers for prognosis and therapeutic response in patients with different cancer types (Ju A. et al., 2021; Lin W. et al., 2021; Shao et al., 2021; Ye et al., 2021). In the current study, we identified the mRNA levels of 52 pyroptosis-related genes in osteosarcoma and normal tissues based on public databases and found that most of these genes were differentially expressed. However, DEPRGs-based consensus clustering analysis produced two clusters that showed no significant differences in clinical characteristics. Subsequently, we performed univariate and LASSO Cox regression analyses to further identify six prognosis-related RPGs. To further explore their biological function and clinical significance, we also performed survival and ROC analyses to develop an accurate pyroptosis-related prognostic signature in osteosarcoma. Subsequently, ssGSEA found that the high-scoring group had lower levels of immune infiltration and fewer immune-related pathways than the low-scoring group. These results suggest that the novel pyroptosis-related genes signature has the potential to predict prognosis accurately and could provide new diagnostic biomarkers and therapeutic targets for patients with osteosarcoma.

As a result of the present study, we constructed a 6-gene pyroptosis-related signature, including BAK1, CASP5, CASP6, GPX4, GZMA, and CHMP4C. Notably, six genes involved in this signature have been implicated in apoptotic pathways as well (Li

et al., 2015; Skotte et al., 2017; Wu et al., 2019; Zhou et al., 2020; Darweesh et al., 2021; Ding et al., 2021). Following apoptotic signals, caspase 8 and caspase 3 initiate pyroptosis by processing GSDMC and GSDME, respectively (Liu et al., 2021). The close relationship between pyroptosis and apoptosis may explain the dual role of these genes. Caspase 5 is an essential player in canonical or noncanonical inflammasome-induced pyroptosis. Upon activation, caspase-5 can act on the GSDMD, leading to the formation of cell membrane pores. Activated caspase-5 can also interact with caspase-1 to promote its activation, and the latter cleaves the precursors of IL-1 $\alpha$  and IL-18 to form active IL-1 $\alpha$  and IL-18, which are released through the channels formed by GSDMD-cNT and lead to pyroptosis (Kayagaki et al., 2015; Xia et al., 2019). Studies have reported that caspase-5 is associated with various malignancies, including gastric cancer, cervical cancer, lung cancer, and human glioblastoma (Babas et al., 2010; Zhou et al., 2018; Wang et al., 2019). Caspase-6 plays a vital role in promoting cell death, ZBP1-mediated inflammasome activation, and host defense during IAV infection (Zheng et al., 2020; Zheng and Kanneganti, 2020). In addition, caspase-6 can also be involved in cancer progression by regulating tumor apoptosis and metastasis (Capo-Chichi et al., 2018). GPX4 was found to negatively regulate Gasdermin D-mediated pyroptosis in lethal polymicrobial sepsis by reducing lipid peroxidation; in contrast, conditional GPX4 knockdown in myeloid cells triggers macrophage pyroptosis with caspase-1/caspase-11-GSDMD-phospholipase C gamma 1 axis. (Kang et al., 2018). Chen et al. (2021a) found that circKIF4A promoted papillary thyroid tumors by sponging miR-1231 and upregulating GPX4 expression. GPX4 is also a ferroptosis-related factor playing an essential role in iron-dependent oxidative cell death driven by lipid peroxidation (Chen X. et al., 2021). Lin H. et al. (2021) discovered that upregulation of HMOX1 to inhibit GPX4 expression induced ferroptosis in osteosarcoma cells by increasing reactive oxygen species levels, malondialdehyde levels, and intracellular ferric ion level. GZMA from cytotoxic lymphocytes enhances antitumor immunity and promotes tumor clearance by cleavage of GSDMB triggering pyroptosis (Zhou et al., 2020). On the other hand, GZMA acts as a pro-inflammatory cytokine to promote cancer development (van Daalen et al., 2020); for instance, GZMA deficiency inhibits colon cancer development and inflammatory response in colon tissue through the NF- $\kappa$ B-IL-6-pSTAT3 axis (Santiago et al., 2020). The polymorphism of CHMP4C increased the cancer susceptibility and was imbalanced in many cancers, including lung, ovarian, prostate, and cervical cancers (Lin S. L. et al., 2020). Another study showed that CHMP4C is also an autophagy-related gene, and its participation in the construction of risk models could effectively predict the prognosis of cervical cancer patients and help develop precise treatment strategies (Shi et al., 2020). Notably, similar to CHMP4C, BAK1 was found to be an apoptosis and pyroptosis-related gene (Cowan et al., 2020; Deo et al., 2020). BAK1 is a member of the Bcl-2 family and can induce mitochondria-mediated apoptosis via regulating the release of cytochrome c (Vervliet et al., 2016). Recent studies have shown that miR-125b, miR-410, and miR-103a-3p could all directly target BAK1 to inhibit apoptosis, and upregulation of BAK1

may contribute to the treatment of cisplatin-resistant non-small cell lung cancer (Wen et al., 2018; Wang H. et al., 2021; Zhang et al., 2021). A prognostic signature based on 14 genes, including BAK1, was able to predict the survival outcome for patients with osteosarcoma (Qi et al., 2021). We also found that PYCARD, although not included in the construction of the model, was also associated with patient outcomes. PYCARD is an adaptor protein that helps form inflammasomes, which contribute to inflammation by promoting the release of the active IL-1 $\beta$  and IL-18 (Hoffman and Wanderer, 2010; Protti and De Monte, 2020). Inflammation is commonly thought to contribute to driving tumor growth, metastasis, and immune escape; for example, IL-1 promotes tumor angiogenesis, recruitment of myeloid cells and contributes to tumor metastasis by recognizing endothelial cell adhesion molecules (Mantovani et al., 2018; Karin and Shalapour, 2021). On the other hand, PYCARD was found to be silenced by promoter methylation in various cancer cells, suggesting its anti-tumor role as a pro-apoptotic factor (Agrawal and Jha, 2020). These studies further confirmed the potential prognostic value of the identified pyroptosis-related genes in osteosarcoma. However, the exact mechanism of their involvement in pyroptosis in osteosarcoma needs to be verified by further *in vivo* and *in vitro* experiments.

The enrichment analysis results showed that the DEGs between high and low PRS-score subgroups were mainly enriched in interferon-gamma mediated signaling pathways, antigen processing, and peptide antigens presented via MHC class II, peptide binding. The MHC-II is the critical component of adaptive anti-tumor immunity, and its upregulation is closely associated with increased levels of interferon-gamma in tumors (Dubrot et al., 2014; Cook et al., 2021). During inflammation, epithelial cells could act as accessory antigen-presenting cells along with the expression of MHC-II (Ghasemi et al., 2020). Tumor-specific MHC-II expression is associated with better prognosis, T-cell infiltration, higher levels of Th1 cytokines, and sensitivity to anti-PD-1 therapies (Johnson et al., 2020). Lu et al. (2017), used the adoptive transfer of MHC-II-restricted tumor-reactive T cells in patients with metastatic cancer (which contained patients with osteosarcoma) and achieved different degrees of tumor regressions in these patients. Coincidentally, the ssGSEA results indicated lower levels of principal anti-tumor infiltrating immune cells in the high PRS-score group, providing further evidence that these genes may play a role in anti-tumor immunity. Studies have shown that chimeric antigen receptor T-cell immunotherapy, a potent option for drug-resistant tumors, has transformed the treatment of drug-resistant hematologic malignancies yet remains largely ineffective against solid tumors, which may be related to the tumor immune microenvironment, the stromal barrier, and the lack of surface tumor-specific targets (Titov et al., 2021). Therefore, we used the ESTIMATE algorithm to examine the distribution of immune scores, stromal scores, and tumor purity in osteosarcoma patients in high and low PRS-score groups. We found that the low-scoring group showed higher immune scores, ESTIMATE scores. Consistent with these results, the high-scoring group had high tumor purity. The PRS-score may help assess the immune microenvironment features of patients and thus predict their

sensitivity to immunotherapy, which will help to guide individualized anti-tumor treatment strategies. Finally, we evaluated the differences in immune checkpoint expression between the two subgroups to determine whether patients would benefit from immune checkpoint inhibitor therapy.

In previous studies, several prognostic signatures have been constructed from different perspectives to predict the prognosis of osteosarcoma. Jiang et al. (2021) created a hypoxia gene-based signature to predict the survival in childhood osteosarcoma. Wang et al. developed a new classification system of osteosarcoma based on immune features and identified TYROBP as a key immune regulatory gene (Wang X. et al., 2021). Qi et al. identified a prognostic signature of osteosarcoma based on 14 autophagy-related genes that can guide clinical decisions in treating osteosarcoma (Qi et al., 2021). Nonetheless, no research has so far concentrated on PRGs-related models, and the current study was designed to fill the vacancy in PRGs-based models for predicting outcomes. Of course, there are inevitably some limitations to this study. Firstly, the verification cohort has a relatively small sample size due to the inherent property of osteosarcoma. Secondly, it lacks experimental work, and the molecular mechanisms of its specific involvement still need further study.

In conclusion, we have developed a novel prognostic model based on six pyroptosis-related genes through comprehensive and systematic bioinformatics analysis, providing an essential foundation for future studies of the association between pyroptosis-related genes and immunity in osteosarcoma.

## DATA AVAILABILITY STATEMENT

The original contributions presented in the study are included in the article/**Supplementary Material**, further inquiries can be directed to the corresponding authors.

## AUTHOR CONTRIBUTIONS

YZ and RH conceived of the research. XL, LM, PJ, and CN collected the data. YZ, RH, XL, XZ, ZY, and CC interpreted the data. YZ and RH drafted the manuscript. DL and QZ critically revised the manuscript. All authors read and approved the final manuscript.

## FUNDING

This work was supported by the National Natural Science Foundation of China (No. 81601931; 81672229), the Natural Science Foundation of Jiangsu Province (BK20150475), the Youth Medical Key Talent Project of Jiangsu (QNRC2016844), “Six One Projects” for high-level health professionals in Jiangsu Province Top Talent Project (LGY2019089), Jiangsu Provincial key research and development program (BE2020679), and the Shenzhen Science and Technology Program (No. KQTD20170810154011370)

## ACKNOWLEDGMENTS

The authors would like to give their sincere appreciation to the reviewers for their helpful comments on this article and research groups for the GTE<sub>x</sub>, TARGET, and CEO, which provided data for this collection.

## REFERENCES

- Agrawal, I., and Jha, S. (2020). Comprehensive Review of ASC Structure and Function in Immune Homeostasis and Disease. *Mol. Biol. Rep.* 47 (4), 3077–3096. doi:10.1007/s11033-020-05345-2
- Babas, E., Ekonomopoulou, M. T., Karapidaki, I., Doxakis, A., Betsas, G., and Iakovidou-Kritsi, Z. (2010). Indication of Participation of Caspase-2 and Caspase-5 in Mechanisms of Human Cervical Malignancy. *Int. J. Gynecol. Cancer* 20 (8), 1381–1385. doi:10.1111/IGC.0b013e3181ed7896
- Bashash, D., Zandi, Z., Kashani, B., Pourbagheri-Sigaroodi, A., Salari, S., and Ghaffari, S. H. (2021). Resistance to Immunotherapy in Human Malignancies: Mechanisms, Research Progresses, Challenges, and Opportunities. *J. Cell Physiol.* [Epub ahead of print]. doi:10.1002/jcp.30575
- Capo-Chichi, C. D., Cai, K. Q., and Xu, X.-X. (2018). Overexpression and Cytoplasmic Localization of Caspase-6 Is Associated with Lamin A Degradation in Set of Ovarian Cancers. *Biomark Res.* 6, 30. doi:10.1186/s40364-018-0144-9
- Chen, W., Fu, J., Chen, Y., Li, Y., Ning, L., Huang, D., et al. (2021a). Circular RNA circKIF4A Facilitates the Malignant Progression and Suppresses Ferroptosis by Sponging miR-1231 and Upregulating GPX4 in Papillary Thyroid Cancer. *Aging* 13 (12), 16500–16512. doi:10.18632/aging.203172
- Chen, X., Yu, C., Kang, R., Kroemer, G., and Tang, D. (2021b). Cellular Degradation Systems in Ferroptosis. *Cell Death Differ* 28 (4), 1135–1148. doi:10.1038/s41418-020-00728-1
- Chow, T., Wutami, I., Lucarelli, E., Choong, P. F., Duchi, S., and Di Bella, C. (2021). Creating *In Vitro* Three-Dimensional Tumor Models: A Guide for the Biofabrication of a Primary Osteosarcoma Model. *Tissue Eng. B: Rev.* 27, 514–529. doi:10.1089/ten.TEB.2020.0254
- Constantinidou, A., Aliferis, C., and Trafalis, D. T. (2019). Targeting Programmed Cell Death -1 (PD-1) and Ligand (PD-L1): A new era in Cancer Active Immunotherapy. *Pharmacol. Ther.* 194, 84–106. doi:10.1016/j.pharmthera.2018.09.008
- Cook, K. W., Xue, W., Symonds, P., Daniels, I., Gijon, M., Boocock, D., et al. (2021). Homocitrullination of Lysine Residues Mediated by Myeloid-Derived Suppressor Cells in the Tumor Environment Is a Target for Cancer Immunotherapy. *J. Immunother. Cancer* 9 (7), e001910. doi:10.1136/jitc-2020-001910
- Cowan, A. D., Smith, N. A., Sandow, J. J., Kapp, E. A., Rustam, Y. H., Murphy, J. M., et al. (2020). BAK Core Dimers Bind Lipids and Can Be Bridged by Them. *Nat. Struct. Mol. Biol.* 27 (11), 1024–1031. doi:10.1038/s41594-020-0494-5
- Darweesh, O., Al-Shehri, E., Falquez, H., Lauterwasser, J., Edlich, F., and Patel, R. (2021). Identification of a Novel Bax-Cdk1 Signalling Complex that Links Activation of the Mitotic Checkpoint to Apoptosis. *J. Cell Sci* 134 (8), jcs244152. doi:10.1242/jcs.244152
- Deo, P., Chow, S. H., Han, M.-L., Speir, M., Huang, C., Schittenhelm, R. B., et al. (2020). Mitochondrial Dysfunction Caused by Outer Membrane Vesicles from Gram-Negative Bacteria Activates Intrinsic Apoptosis and Inflammation. *Nat. Microbiol.* 5 (11), 1418–1427. doi:10.1038/s41564-020-0773-2
- Ding, Y., Chen, X., Liu, C., Ge, W., Wang, Q., Hao, X., et al. (2021). Identification of a Small Molecule as Inducer of Ferroptosis and Apoptosis through Ubiquitination of GPX4 in Triple Negative Breast Cancer Cells. *J. Hematol. Oncol.* 14 (1), 19. doi:10.1186/s13045-020-01016-8
- Dubrot, J., Duraes, F. V., Potin, L., Capotosti, F., Brighouse, D., Suter, T., et al. (2014). Lymph Node Stromal Cells Acquire Peptide-MHCII Complexes from Dendritic Cells and Induce Antigen-specific CD4+ T Cell Tolerance. *J. Exp. Med.* 211 (6), 1153–1166. doi:10.1084/jem.20132000
- Fan, Z., Huang, G., Zhao, J., Li, W., Lin, T., Su, Q., et al. (2021). Establishment and Characterization of a Highly Metastatic Human Osteosarcoma Cell Line from

## SUPPLEMENTARY MATERIAL

The Supplementary Material for this article can be found online at: <https://www.frontiersin.org/articles/10.3389/fgene.2021.780780/full#supplementary-material>

- Osteosarcoma Lung Metastases. *J. Bone Oncol.* 29, 100378. doi:10.1016/j.jbo.2021.100378
- Gazouli, I., Kyriazoglou, A., Kotsantis, I., Anastasiou, M., Pantazopoulos, A., Prevezanou, M., et al. (2021). Systematic Review of Recurrent Osteosarcoma Systemic Therapy. *Cancers* 13 (8), 1757. doi:10.3390/cancers13081757
- Ghasemi, F., Tessier, T. M., Gameiro, S. F., Maciver, A. H., Cecchini, M. J., and Mymryk, J. S. (2020). High MHC-II Expression in Epstein-Barr Virus-Associated Gastric Cancers Suggests that Tumor Cells Serve an Important Role in Antigen Presentation. *Sci. Rep.* 10 (1), 14786. doi:10.1038/s41598-020-17775-4
- Hashimoto, K., Nishimura, S., and Akagi, M. (2020). Characterization of PD-1/pd-L1 Immune Checkpoint Expression in Osteosarcoma. *Diagnostics* 10 (8), 528. doi:10.3390/diagnostics10080528
- Hoffman, H. M., and Wanderer, A. A. (2010). Inflammasome and IL-1 $\beta$ -Mediated Disorders. *Curr. Allergy Asthma Rep.* 10 (4), 229–235. doi:10.1007/s11882-010-0109-z
- Jiang, F., Miao, X.-L., Zhang, X.-T., Yan, F., Mao, Y., Wu, C.-Y., et al. (2021). A Hypoxia Gene-Based Signature to Predict the Survival and Affect the Tumor Immune Microenvironment of Osteosarcoma in Children. *J. Immunol. Res.* 2021, 1–13. doi:10.1155/2021/5523832
- Johnson, A. M., Bullock, B. L., Neuwelt, A. J., Poczobutt, J. M., Kaspar, R. E., Li, H. Y., et al. (2020). Cancer Cell-Intrinsic Expression of MHC Class II Regulates the Immune Microenvironment and Response to Anti-PD-1 Therapy in Lung Adenocarcinoma. *J. Immunol.* 204 (8), 2295–2307. doi:10.4049/jimmunol.1900778
- Ju, A., Tang, J., Chen, S., Fu, Y., and Luo, Y. (2021a). Pyroptosis-Related Gene Signatures Can Robustly Diagnose Skin Cutaneous Melanoma and Predict the Prognosis. *Front. Oncol.* 11, 709077. doi:10.3389/fonc.2021.709077
- Ju, X., Yang, Z., Zhang, H., and Wang, Q. (2021b). Role of Pyroptosis in Cancer Cells and Clinical Applications. *Biochimie* 185, 78–86. doi:10.1016/j.biochi.2021.03.007
- Judge, S. J., Darrow, M. A., Thorpe, S. W., Gingrich, A. A., O'Donnell, E. F., Bellini, A. R., et al. (2020). Analysis of Tumor-Infiltrating NK and T Cells Highlights IL-15 Stimulation and TIGIT Blockade as a Combination Immunotherapy Strategy for Soft Tissue Sarcomas. *J. Immunother. Cancer* 8 (2), e001355. doi:10.1136/jitc-2020-001355
- Kang, R., Zeng, L., Zhu, S., Xie, Y., Liu, J., Wen, Q., et al. (2018). Lipid Peroxidation Drives Gasdermin D-Mediated Pyroptosis in Lethal Polymicrobial Sepsis. *Cell Host & Microbe* 24 (1), 97–108.e4. doi:10.1016/j.chom.2018.05.009
- Karin, M., and Shalapour, S. (2021). Regulation of Antitumor Immunity by Inflammation-Induced Epigenetic Alterations. *Cell Mol Immunol.* [Epub ahead of print]. doi:10.1038/s41423-021-00756-y
- Kayagaki, N., Stowe, I. B., Lee, B. L., O'Rourke, K., Anderson, K., Warming, S., et al. (2015). Caspase-11 Cleaves Gasdermin D for Non-canonical Inflammasome Signalling. *Nature* 526 (7575), 666–671. doi:10.1038/nature15541
- Li, K., Liu, J., Tian, M., Gao, G., Qi, X., Pan, Y., et al. (2015). CHMP4C Disruption Sensitizes the Human Lung Cancer Cells to Irradiation. *Int. J. Mol. Sci.* 17 (1), 18. doi:10.3390/ijms17010018
- Li, L., Jiang, M., Qi, L., Wu, Y., Song, D., Gan, J., et al. (2021a). Pyroptosis, a New Bridge to Tumor Immunity. *Cancer Sci.* 112, 3979–3994. doi:10.1111/cas.15059
- Li, M., Wu, W., Deng, S., Shao, Z., and Jin, X. (2021b). TRAIIP Modulates the IGFBP3/AKT Pathway to Enhance the Invasion and Proliferation of Osteosarcoma by Promoting KANK1 Degradation. *Cell Death Dis* 12 (8), 767. doi:10.1038/s41419-021-04057-0
- Li, L., Li, Y., and Bai, Y. (2020). Role of GSDMB in Pyroptosis and Cancer. *Cancer Manag. Res.* 12, 3033–3043. doi:10.2147/cmar.S246948
- Ligon, J. A., Choi, W., Cojocar, G., Fu, W., Hsiue, E. H.-C., Oke, T. F., et al. (2021). Pathways of Immune Exclusion in Metastatic Osteosarcoma Are Associated with Inferior Patient Outcomes. *J. Immunother. Cancer* 9 (5), e001772. doi:10.1136/jitc-2020-001772

- Lin, H., Chen, X., Zhang, C., Yang, T., Deng, Z., Song, Y., et al. (2021a). EF24 Induces Ferroptosis in Osteosarcoma Cells through HMOX1. *Biomed. Pharmacother.* 136, 111202. doi:10.1016/j.biopha.2020.111202
- Lin, W., Chen, Y., Wu, B., Chen, Y., and Li, Z. (2021b). Identification of the Pyroptosis-related Prognostic Gene Signature and the Associated Regulation Axis in Lung Adenocarcinoma. *Cell Death Discov.* 7 (1), 161. doi:10.1038/s41420-021-00557-2
- Lin, R., Wei, H., Wang, S., Huang, Z., Chen, H., Zhang, S., et al. (2020a). Gasdermin D Expression and Clinicopathologic Outcome in Primary Osteosarcoma Patients. *Int. J. Clin. Exp. Pathol.* 13 (12), 3149–3157.
- Lin, S. L., Wang, M., Cao, Q. Q., and Li, Q. (2020b). Chromatin Modified Protein 4C (CHMP4C) Facilitates the Malignant Development of Cervical Cancer Cells. *FEBS Open Bio* 10 (7), 1295–1303. doi:10.1002/2211-5463.12880
- Liu, X., Xia, S., Zhang, Z., Wu, H., and Lieberman, J. (2021). Channelling Inflammation: Gasdermins in Physiology and Disease. *Nat. Rev. Drug Discov.* 20 (5), 384–405. doi:10.1038/s41573-021-00154-z
- Lovless, R., Bloomquist, R., and Teng, Y. (2021). Pyroptosis at the Forefront of Anticancer Immunity. *J. Exp. Clin. Cancer Res.* 40 (1), 264. doi:10.1186/s13046-021-02065-8
- Lu, X., Guo, T., and Zhang, X. (2021). Pyroptosis in Cancer: Friend or Foe? *Cancers* 13 (14), 3620. doi:10.3390/cancers13143620
- Lu, Y.-C., Parker, L. L., Lu, T., Zheng, Z., Toomey, M. A., White, D. E., et al. (2017). Treatment of Patients with Metastatic Cancer Using a Major Histocompatibility Complex Class II-Restricted T-Cell Receptor Targeting the Cancer Germline Antigen MAGE-A3. *J. Clin. Oncol.* 35 (29), 3322–3329. doi:10.1200/jco.2017.74.5463
- Mantovani, A., Barajon, I., and Garlanda, C. (2018). IL-1 and IL-1 Regulatory Pathways in Cancer Progression and Therapy. *Immunol. Rev.* 281 (1), 57–61. doi:10.1111/imr.12614
- Na, Z., Fan, L., and Wang, X. (2021). Gene Signatures and Prognostic Values of N6-Methyladenosine Related Genes in Ovarian Cancer. *Front. Genet.* 12, 542457. doi:10.3389/fgene.2021.542457
- Ni, S., Li, J., Qiu, S., Xie, Y., Gong, K., and Duan, Y. (2020). KIF21B Expression in Osteosarcoma and its Regulatory Effect on Osteosarcoma Cell Proliferation and Apoptosis through the PI3K/AKT Pathway. *Front. Oncol.* 10, 606765. doi:10.3389/fonc.2020.606765
- Pan, J., Zhang, X., Fang, X., and Xin, Z. (2021). Construction of a Ferroptosis-Related lncRNA-Based Model to Improve the Prognostic Evaluation of Gastric Cancer Patients Based on Bioinformatics. *Front. Genet.* 12, 739470. doi:10.3389/fgene.2021.739470
- Park, J. A., and Cheung, N.-K. V. (2020). GD2 or HER2 Targeting T Cell Engaging Bispecific Antibodies to Treat Osteosarcoma. *J. Hematol. Oncol.* 13 (1), 172. doi:10.1186/s13045-020-01012-y
- Protti, M. P., and De Monte, L. (2020). Dual Role of Inflammasome Adaptor ASC in Cancer. *Front. Cell Dev. Biol.* 8, 40. doi:10.3389/fcell.2020.00040
- Qi, W., Yan, Q., Lv, M., Song, D., Wang, X., and Tian, K. (2021). Prognostic Signature of Osteosarcoma Based on 14 Autophagy-Related Genes. *Pathol. Oncol. Res.* 27, 1609782. doi:10.3389/pore.2021.1609782
- Rojas, G. A., Hubbard, A. K., Diessner, B. J., Ribeiro, K. B., and Spector, L. G. (2021). International Trends in Incidence of Osteosarcoma (1988–2012). *Int. J. Cancer* 149 (5), 1044–1053. doi:10.1002/ijc.33673
- Santiago, L., Castro, M., Sanz-Pamplona, R., Garzón, M., Ramirez-Labrada, A., Tapia, E., et al. (2020). Extracellular Granzyme A Promotes Colorectal Cancer Development by Enhancing Gut Inflammation. *Cel Rep.* 32 (1), 107847. doi:10.1016/j.celrep.2020.107847
- Shao, W., Yang, Z., Fu, Y., Zheng, L., Liu, F., Chai, L., et al. (2021). The Pyroptosis-Related Signature Predicts Prognosis and Indicates Immune Microenvironment Infiltration in Gastric Cancer. *Front. Cell Dev. Biol.* 9, 676485. doi:10.3389/fcell.2021.676485
- Shi, H., Zhong, F., Yi, X., Shi, Z., Ou, F., Xu, Z., et al. (2020). Application of an Autophagy-Related Gene Prognostic Risk Model Based on TCGA Database in Cervical Cancer. *Front. Genet.* 11, 616998. doi:10.3389/fgene.2020.616998
- Shin, C., Kim, S. S., and Jo, Y. H. (2021). Extending Traditional Antibody Therapies: Novel Discoveries in Immunotherapy and Clinical Applications. *Mol. Ther. - Oncolytics* 22, 166–179. doi:10.1016/j.omto.2021.08.005
- Skotte, N. H., Sanders, S. S., Singaraja, R. R., Ehrnhoefer, D. E., Vaid, K., Qiu, X., et al. (2017). Palmitoylation of Caspase-6 by HIP14 Regulates its Activation. *Cel Death Differ* 24 (3), 433–444. doi:10.1038/cdd.2016.139
- Subramanian, A., Tamayo, P., Mootha, V. K., Mukherjee, S., Ebert, B. L., Gillette, M. A., et al. (2005). Gene Set Enrichment Analysis: a Knowledge-Based Approach for Interpreting Genome-wide Expression Profiles. *Proc. Natl. Acad. Sci.* 102 (43), 15545–15550. doi:10.1073/pnas.0506580102
- Tang, Z., Ji, L., Han, M., Xie, J., Zhong, F., Zhang, X., et al. (2020). Pyroptosis Is Involved in the Inhibitory Effect of FL118 on Growth and Metastasis in Colorectal Cancer. *Life Sci.* 257, 118065. doi:10.1016/j.lfs.2020.118065
- Titov, A., Zmievskaia, E., Ganeeva, I., Valiullina, A., Petukhov, A., Rakhmatullina, A., et al. (2021). Adoptive Immunotherapy beyond CAR T-Cells. *Cancers* 13 (4), 743. doi:10.3390/cancers13040743
- van Daalen, K. R., Reijneveld, J. F., and Bovenschen, N. (2020). Modulation of Inflammation by Extracellular Granzyme A. *Front. Immunol.* 11, 931. doi:10.3389/fimmu.2020.00931
- Vervliet, T., Parys, J. B., and Bultynck, G. (2016). Bcl-2 Proteins and Calcium Signaling: Complexity beneath the Surface. *Oncogene* 35 (39), 5079–5092. doi:10.1038/onc.2016.31
- Wang, H., Huang, H., Wang, L., Liu, Y., Wang, M., Zhao, S., et al. (2021a). Cancer-associated Fibroblasts Secreted miR-103a-3p Suppresses Apoptosis and Promotes Cisplatin Resistance in Non-small Cell Lung Cancer. *Aging* 13 (10), 14456–14468. doi:10.18632/aging.103556
- Wang, X., Wang, L., Xu, W., Wang, X., Ke, D., Lin, J., et al. (2021b). Classification of Osteosarcoma Based on Immunogenomic Profiling. *Front. Cell Dev. Biol.* 9, 696878. doi:10.3389/fcell.2021.696878
- Wang, S.-D., Li, H.-Y., Li, B.-H., Xie, T., Zhu, T., Sun, L.-L., et al. (2016a). The Role of CTLA-4 and PD-1 in Anti-tumor Immune Response and Their Potential Efficacy against Osteosarcoma. *Int. Immunopharmacol.* 38, 81–89. doi:10.1016/j.intimp.2016.05.016
- Wang, Y., Kong, H., Zeng, X., Liu, W., Wang, Z., Yan, X., et al. (2016b). Activation of NLRP3 Inflammasome Enhances the Proliferation and Migration of A549 Lung Cancer Cells. *Oncol. Rep.* 35 (4), 2053–2064. doi:10.3892/or.2016.4569
- Wang, W. J., Chen, D., Jiang, M. Z., Xu, B., Li, X. W., Chu, Y., et al. (2018). Downregulation of Gasdermin D Promotes Gastric Cancer Proliferation by Regulating Cell Cycle-Related Proteins. *J. Dig. Dis.* 19 (2), 74–83. doi:10.1111/1751-2980.12576
- Wang, Z., Ni, F., Yu, F., Cui, Z., Zhu, X., and Chen, J. (2019). Prognostic Significance of mRNA Expression of CASPs in Gastric Cancer. *Oncol. Lett.* 18 (5), 4535–4554. doi:10.3892/ol.2019.10816
- Wen, R., Umeano, A. C., Essegian, D. J., Sabitaliyevich, U. Y., Wang, K., and Farooqi, A. A. (2018). Role of microRNA-410 in Molecular Oncology: A Double Edged Sword. *J. Cel Biochem* 119 (11), 8737–8742. doi:10.1002/jcb.27251
- Wu, D., Wei, C., Li, Y., Yang, X., and Zhou, S. (2021). Pyroptosis, a New Breakthrough in Cancer Treatment. *Front. Oncol.* 11, 698811. doi:10.3389/fonc.2021.698811
- Wu, Y., Zhuang, J., Zhao, D., and Xu, C. (2019). Interaction between Caspase-3 and Caspase-5 in the Stretch-induced Programmed Cell Death in the Human Periodontal Ligament Cells. *J. Cel Physiol* 234 (8), 13571–13581. doi:10.1002/jcp.28035
- Xia, X., Wang, X., Cheng, Z., Qin, W., Lei, L., Jiang, J., et al. (2019). The Role of Pyroptosis in Cancer: Pro-cancer or Pro-"host"? *Cel Death Dis* 10 (9), 650. doi:10.1038/s41419-019-1883-8
- Xing, X., Gu, F., Hua, L., Cui, X., Li, D., Wu, Z., et al. (2021). TIMELESS Promotes Tumor Progression by Enhancing Macrophages Recruitment in Ovarian Cancer. *Front. Oncol.* 11, 732058. doi:10.3389/fonc.2021.732058
- Yao, Q., and Chen, T. (2020). LINC01128 Regulates the Development of Osteosarcoma by Sponging miR-299-3p to Mediate MMP2 Expression and Activating Wnt/ $\beta$ -catenin Signalling Pathway. *J. Cel. Mol. Med.* 24 (24), 14293–14305. doi:10.1111/jcmm.16046
- Ye, Y., Dai, Q., and Qi, H. (2021). A Novel Defined Pyroptosis-Related Gene Signature for Predicting the Prognosis of Ovarian Cancer. *Cel Death Discov.* 7 (1), 71. doi:10.1038/s41420-021-00451-x
- Zhang, B., Mao, S., Liu, X., Li, S., Zhou, H., Gu, Y., et al. (2021). MiR-125b Inhibits Cardiomyocyte Apoptosis by Targeting BAK1 in Heart Failure. *Mol. Med.* 27 (1), 72. doi:10.1186/s10020-021-00328-w
- Zheng, M., and Kanneganti, T. D. (2020). The Regulation of the ZBP1-NLRP3 Inflammasome and its Implications in Pyroptosis, Apoptosis, and Necroptosis (PANoptosis). *Immunol. Rev.* 297 (1), 26–38. doi:10.1111/imr.12909

- Zheng, M., Karki, R., Vogel, P., and Kanneganti, T.-D. (2020). Caspase-6 Is a Key Regulator of Innate Immunity, Inflammasome Activation, and Host Defense. *Cell* 181 (3), 674–687.e13. doi:10.1016/j.cell.2020.03.040
- Zhou, C.-B., and Fang, J.-Y. (2019). The Role of Pyroptosis in Gastrointestinal Cancer and Immune Responses to Intestinal Microbial Infection. *Biochim. Biophys. Acta (Bba) - Rev. Cancer* 1872 (1), 1–10. doi:10.1016/j.bbcan.2019.05.001
- Zhou, Y., Dai, W., Wang, H., Pan, H., and Wang, Q. (2018). Long Non-coding RNA CASP5 Promotes the Malignant Phenotypes of Human Glioblastoma Multiforme. *Biochem. Biophysical Res. Commun.* 500 (4), 966–972. doi:10.1016/j.bbrc.2018.04.217
- Zhou, Z., He, H., Wang, K., Shi, X., Wang, Y., Su, Y., et al. (2020). Granzyme A from Cytotoxic Lymphocytes Cleaves GSDMB to Trigger Pyroptosis in Target Cells. *Science* 368 (6494), eaaz7548. doi:10.1126/science.aaz7548

**Conflict of Interest:** Author QZ was employed by the company Shenzhen Tyercan Bio-Pharm Co., Ltd.

The remaining authors declare that the research was conducted in the absence of any commercial or financial relationships that could be construed as a potential conflict of interest.

**Publisher's Note:** All claims expressed in this article are solely those of the authors and do not necessarily represent those of their affiliated organizations, or those of the publisher, the editors and the reviewers. Any product that may be evaluated in this article, or claim that may be made by its manufacturer, is not guaranteed or endorsed by the publisher.

Copyright © 2021 Zhang, He, Lei, Mao, Jiang, Ni, Yin, Zhong, Chen, Zheng and Li. This is an open-access article distributed under the terms of the Creative Commons Attribution License (CC BY). The use, distribution or reproduction in other forums is permitted, provided the original author(s) and the copyright owner(s) are credited and that the original publication in this journal is cited, in accordance with accepted academic practice. No use, distribution or reproduction is permitted which does not comply with these terms.